Spontaneous Formation of Surface Antisite Defects in the Stabilization of the Sb-Rich GaSb(001) Surface

Conor Hogan,[1,*] Rita Magri,[2] and Rodolfo Del Sole[1]

[1]*European Theoretical Spectroscopy Facility (ETSF), CNR-INFM-SMC, and Dipartimento di Fisica,
Università di Roma "Tor Vergata," Via della Ricerca Scientifica 1, 00133 Roma, Italy*
[2]*Centro S3, CNR-Istituto di Nanoscienze and Dipartimento di Fisica, Università di Modena e Reggio Emilia,
Via Campi 213/A, I-41100 Modena, Italy*
(Received 23 June 2009; published 14 April 2010)

This Letter solves the long-standing puzzle [Phys. Rev. Lett. **79,** 693 (1997)] of why GaSb(001) apparently violates the electron counting rule (ECR) in forming a reconstruction featuring long Sb-dimer chains, rather than the $c(4 \times 4)$ reconstruction found in all other arsenide and antimonide III–V compounds in the V-rich regime. We find that an alternative strategy, that in fact satisfies the ECR, is followed by the Sb-rich GaSb(001) surface, whereby long Sb-dimer chains are stabilized by randomly distributed subsurface Ga antisite defects. The excess of surface Sb drives the defect formation that in turn stabilizes the surface in a metastable phase. The transition to the $c(4 \times 4)$ reconstruction, where the ECR is instead satisfied through missing dimers, is therefore inhibited. Our conclusions are supported by *ab initio* simulations of experimental reflectance anisotropy spectra.

The basic maxim of semiconductor surface formation states that surfaces tend to reconstruct and relax so as to have the lowest surface energy possible [1]. A well known principle that encapsulates this is the electron counting rule (ECR). In the case of the III–V compound semiconductors that form the basis of several wireless and optoelectronics technologies, this rule affirms that the lowest energy reconstructions are those having empty dangling bonds on the cations (III), and filled dangling bonds on the anions (V). As a consequence, no surface states cross the Fermi energy, and the surface is semiconducting. In fact, the ECR is fulfilled by almost all low energy reconstructions observed so far.

The Sb-rich GaSb(001) surface is often cited as the archetypal case of a simple clean surface where the ECR is *not* fulfilled [2]. Scanning tunnelling microscopy (STM) images of this surface show long unbroken Sb-dimer chains [2–4], and scanning tunnelling spectroscopy (STS) studies reveal a weak metallicity [2]. The proposed structures break the ECR and theoretical calculations confirm that they are energetically unstable. Why this surface forms has remained a mystery of surface science and questions the wider applicability of the ECR.

In this Letter, we provide conclusive evidence, by means of accurate *ab initio* total energy calculations, that GaSb(001) follows an alternative strategy for stabilizing anion-rich surfaces that is not followed by any of the other arsenide and antimonide III–Vs. In this alternative route, the system is stabilized by the random substitution of subsurface Sb atoms with Ga atoms, which can happen if the Sb-rich surface has a low enough strain to easily accommodate Sb dimers (and thus become electron rich). These defects lower the excess surface electronic charge,

facilitating the formation of long dimer chains. The strategy allows the ECR to be obeyed, and the surface to become, on the whole, semiconducting. It is demonstrated to occur (at least) on Sb-rich GaSb(001), indicating that the ECR is *not*, on the whole, violated. Our conclusions are supported by *ab initio* simulations of previously reported experimental reflectance anisotropy (RA) spectra.

In the V-rich regime, the majority of III–Vs form the well-known $c(4 \times 4)$ reconstruction. This may be considered as an array of closely packed infinite dimer chains having every fourth dimer missing: as a result, chains only three dimers long are present on the surface [see Fig. 1(a)]. In contrast, scanning tunnelling measurements of GaSb(001) suggest that the Sb-rich surface is composed of long single or double dimer rows separated by *in-dimers* of Sb [2]. The resulting $c(2 \times 10)$ reconstruction having double dimer rows [see Fig. 1(b)] is unique to GaSb. The analogous structure for the $c(2 \times 6)$ phase having a single dimer row is also shown in Fig. 1(b). At intermediate Sb coverages, GaSb forms a mixture of (4×3) reconstructions (yielding an overall (1×3) symmetry) [5,6], an example of which, $h0(4 \times 3)$, is shown in Fig. 1(a). It is well established that (4×3) phases are the most stable ones in GaSb [7,8], and the α and β variations have been indeed observed by STM [5].

In order to clarify the structures and stability of the diverse GaSb(001) reconstructions, we employed density functional theory in the local density approximation (DFT-LDA) in a plane-wave framework using norm-conserving pseudopotentials [9]. We performed total energy calculations for these reconstructions on GaSb and computed the surface energy γ in the usual way [10] as a function of $\Delta \mu_{Sb} = \mu_{Sb} - \mu_{Sb}^{bulk}$, i.e., the difference between the ac-
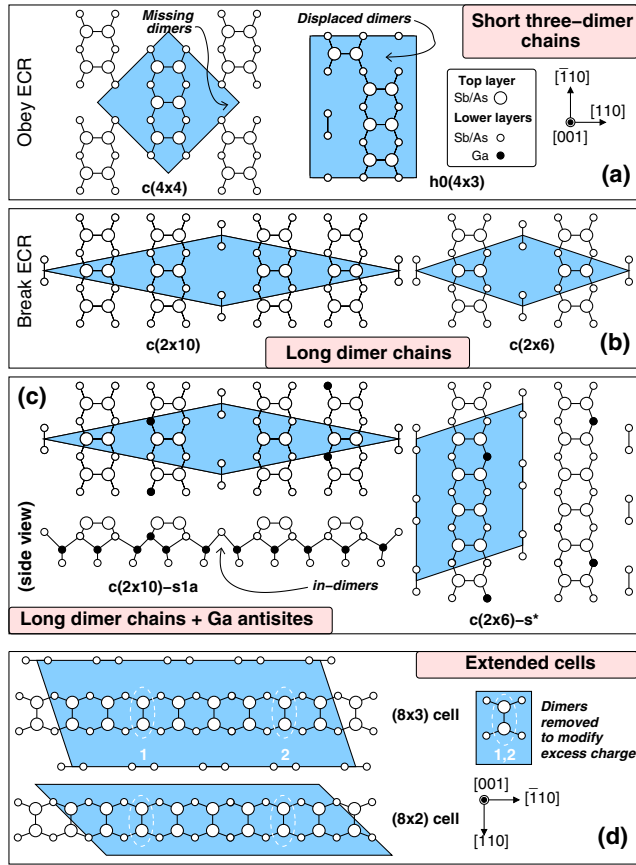
FIG. 1 (color online).   (a)–(c) Ball-and-stick models of V-rich III–V(001) reconstructions (top view, unless specified otherwise). Panel (d) shows extended cells (axes rotated by 90°) containing long dimer chains, closely spaced [(8×2)] or separated by in-dimers [(8×3)]. Shaded regions define primitive surface unit cells.

FIG. 2 (color online).   Surface phase diagram for GaSb(001). Surface energies γ are plotted relative to the $\alpha(4 \times 3)$ reconstruction.

tual value of the Sb chemical potential with respect to that of elemental bulk Sb in the rhombohedral $A7$ phase. The resulting surface phase diagram is shown in Fig. 2. We confirm earlier results [7,11] that showed structures based on infinite dimer chains, i.e., those in Fig. 1(b), to be relatively high in energy. This instability can be directly ascribed to the fact that they violate the ECR, rendering them metallic.

To explore possible stabilization mechanisms for the observed long-chain reconstructions, we introduce acceptorlike defects to compensate the surface electron excess. We consider variations of the long chain models in which *second* row Sb atoms are substituted by Ga atoms, henceforth referred to as surface Ga antisite defects. In contrast to bulk Ga antisites, these surface Ga antisites form two Ga–Ga bonds and two Ga–Sb bonds. Such defects were proposed by Houze *et al.* [11] as a way to reduce the metallicity of the long dimer chains occurring in the $c(2 \times 10)$ surface. The most stable structure identified in that work, $c(2 \times 10)$-$s1a$, is shown in Fig. 1(c). Here, we extend this "doping" model to exactly satisfy the ECR
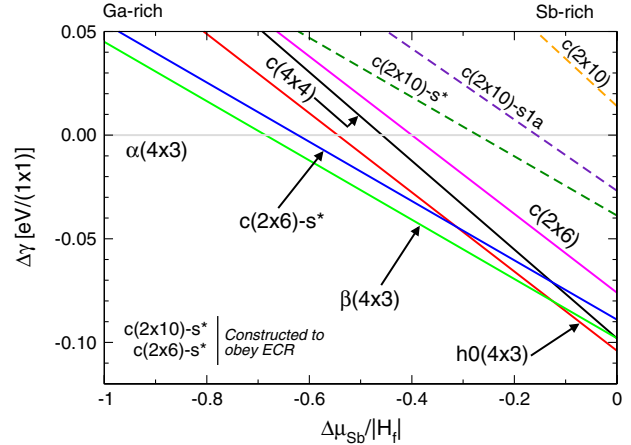
in both the $c(2 \times 10)$ and $c(2 \times 6)$ phases by inserting the correct density of surface Ga antisites in each case [a typical "$c(2 \times 6)$-$s*$" structure is shown in Fig. 1(c)]. We find that these new structures are indeed far more stable than the metallic ones, as shown in Fig. 2. Nevertheless, their energy is still above that of the ground state (4×3) structures. Therefore, our calculations show that the phases stabilized by surface Ga defects are metastable, and should be determined by the particular preparation conditions.

GaSb(001) is unique among the III–Vs by having the closest lattice matching (0.30% mismatch) to the crystalline V element phase [2], as evidenced by the fact that GaSb can be capped with polycrystalline—i.e., not amorphous—Sb [12]. Other III–V compounds, in contrast, show mismatches greater than 6% (the exception being AlSb, with a small mismatch of 0.97%). This unique property of GaSb makes the formation of Sb dimers particularly favorable, leading to electron-rich regions of surface charge. We now demonstrate that these electron-rich conditions trigger spontaneous formation of the subsurface defects.

First, we note that the number of excess electrons ν (that is, the electrons left over when all available bonds and Sb dangling bonds are filled) is directly related to the concentration of each possible structural motif appearing on the (001) surface (see Fig. 1). For the ECR to be fulfilled and the system semiconducting, ν must equal zero. We considered extended cells that are initially composed of long dimer chains separated by in-dimers [the (8×3) cells] or not [(8×2) cells] [see Fig. 1(d)]. Note that this initial (8×3) structure is precisely equivalent to the usual $c(2 \times 6)$ phase. These unbroken chain structures correspond to the largest possible value of ν for each cell type and have their Fermi levels lying inside the conduction band. We then systematically reduced ν by removing dimers from the dimer chain, thus lowering the Fermi level into the gap. For each configuration (i.e., each value of ν), we determined the defect formation energy (DFE) of a single Ga antisite as

$$\mathrm{DFE} = A(\gamma_{\mathrm{phase+defect}} - \gamma_{\mathrm{phase}})$$

$$= E_{\mathrm{phase+defect}} - E_{\mathrm{phase}} + \mu_{\mathrm{Sb}} - \mu_{\mathrm{Ga}},$$

where A is the cell area. Taking into account that $\mu_{\mathrm{Sb}} + \mu_{\mathrm{Ga}} = \mu_{\mathrm{GaSb}}^{\mathrm{bulk}}$ and $\mu_{\mathrm{GaSb}}^{\mathrm{bulk}} - \mu_{\mathrm{Ga}}^{\mathrm{bulk}} - \mu_{\mathrm{Sb}}^{\mathrm{bulk}} = H_f$, where H_f is the GaSb bulk compound formation energy, we obtain

$$\mathrm{DFE} = E_{\mathrm{phase+defect}} - E_{\mathrm{phase}} + \mu_{\mathrm{Sb}}^{\mathrm{bulk}} - \mu_{\mathrm{Ga}}^{\mathrm{bulk}} - H_f$$

$$+ 2\Delta\mu_{\mathrm{Sb}}.$$

Values for $\mathrm{DFE}(\nu, \Delta\mu_{\mathrm{V}})$ computed in this way for GaSb(001), GaAs(001), and AlSb(001) are shown in Fig. 3(a). The solid dots correspond to DFE at $\Delta\mu_{\mathrm{V}}/|H_f| = 0$, while the "error" bars describe the variation of DFE over the range $-0.3 < \Delta\mu_{\mathrm{V}}/|H_f| < 0$ (the high-V regime). It is apparent from Fig. 3(a) that defect formation occurs spontaneously (DFE < 0) for GaSb(001) as soon as ν exceeds 0.14 electrons per (1×1) cell. This shows that exchange of a subsurface Sb atom with a Ga atom can result from a fluctuation in the surface electron number. From the figure, we can also see that the defect is quite stable in the $c(2 \times 6)$-$s*$ ($\nu = 0.167$) and $c(2 \times 10)$-$s1a$ ($\nu = 0.3$) structures. This spontaneous for-

FIG. 3 (color online). (a) Surface Ga antisite defect formation energy (DFE) as a function of the number of excess electrons ν. Points marked $c(2 \times 10)$-$s1a$ and $c(2 \times 6)$-$s*$ indicate the average defect energies of these structures. The numbers in parenthesis indicate dimers removed from initial extended cells. (b) Surface energies of GaSb and GaAs(001) metallic chains, compared with those of chains modified to obey the ECR by means of removal of dimers or addition of defects.

mation of defects on Sb-rich GaSb(001) stabilizes the long Sb-dimer chain metastable structures observed in the experiments and inhibits the phase transition to the $c(4 \times 4)$ reconstruction. In GaAs(001) and AlSb(001), the DFE always remains positive so that defect formation is not favored. These surfaces must therefore stabilize through the usual strategy of removing dimers, and indeed are experimentally observed to form the $c(4 \times 4)$ reconstruction in the very V-rich regime. AlSb(001) is particularly interesting since AlSb is almost lattice-matched to GaSb and the (001) surface forms the same (1×3) reconstructions at lower Sb coverages.

Next, we compare the surface energies obtained when two different mechanisms for satisfying the ECR are followed: (i) exchange of subsurface V atoms with Ga (formation of surface Ga antisites) and (ii) formation of missing dimers. Again, we consider both (8×3)- and (8×2)-type cells, to account for the possibility that in-dimers may or may not be present on the III–V(001) surface. In the case of the (8×3) cell, the ECR is fulfilled if one dimer is removed or two surface Ga antisites added, whereas for the (8×2) cell, two dimers must be removed or four antisites added. Note that removing two dimers from the (8×2) cell (from the positions indicated in Fig. 1) results in the usual $c(4 \times 4)$ reconstruction.

Surface energies of the resulting structures are shown in Fig. 3(b) for GaSb(001) and GaAs(001). In fact, the data corresponding to infinite chains with and without Ga antisites in the (8×2) cell are too high in energy to be plotted. In the case of GaSb(001), the reconstruction having two antisites in the (8×3) cell has a lower surface energy at *all* Sb chemical potentials than the (8×3) reconstruction missing one dimer. Hence, in the presence of an excess of Sb dimers, the system tends to fulfil the ECR via formation of Ga antisites, keeping the dimer rows unchanged. This strategy stabilizes long dimer chains and prevents the transition to the $c(4 \times 4)$ phase. In contrast, Fig. 3(b) shows that this route will never be followed by GaAs(001), since antisite formation is clearly unfavored and the $c(4 \times 4)$ reconstruction is by far the more stable (notice the different vertical scale in the figure), as is expected.

Our calculations also show that (i) the interaction between antisites raises the system energy, and thus they tend to spread out, and (ii) the total energies of structures having the same concentration of Ga antisites, but distributed differently about the surface [subject to condition (i)], are very similar. Thus, we expect a random distribution of antisites, recovering the overall symmetry of the long-chain structures [$c(2 \times 6)$ and $c(2 \times 10)$]. Local fluctuations in the Ga antisite concentration may explain the weak metallicity observed with STS (a local probe) on the $c(2 \times 10)$ surface [2]: even if the ECR is globally satisfied, the structural disorder ensures that it can be locally violated.

Indirect experimental evidence for the formation of these defects was provided by Houze *et al.* [11], who inferred that the observed asymmetry of top layer Sb dimer
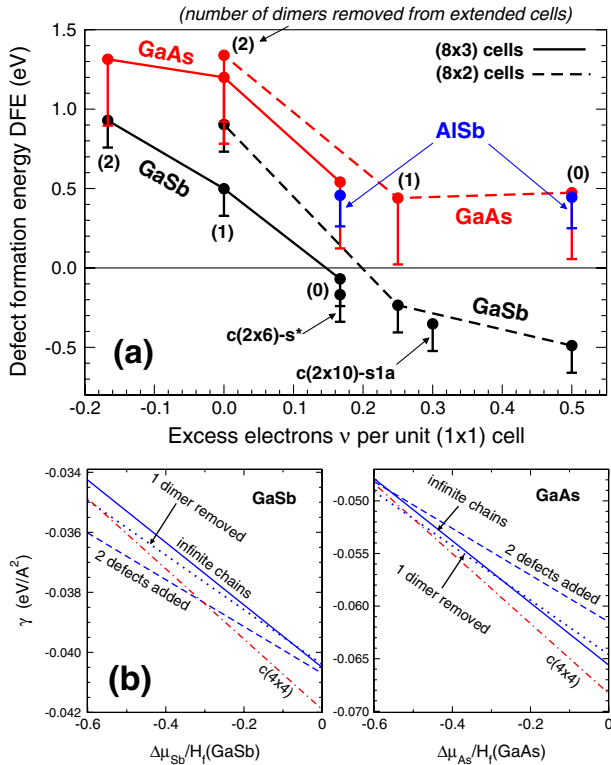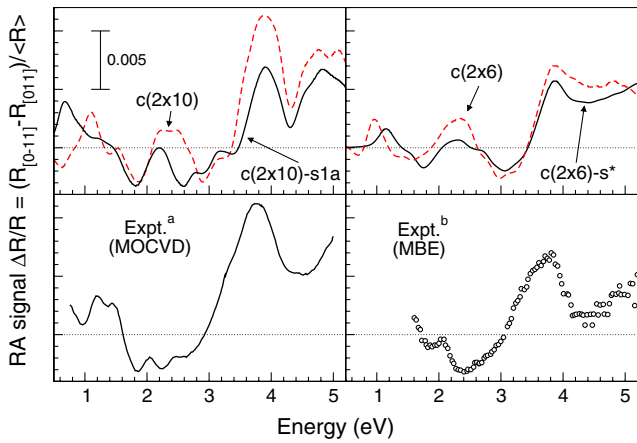
FIG. 4 (color online). Reflectance anisotropy spectra of GaSb (001). Top: calculated spectra, with and without Ga antisites. Bottom: experimental spectra, taken from Refs. [14] (a) and [12] (b).

in STM images of the $c(2 \times 10)$ phase [2] was due to the presence of Ga atoms in the second layer. Here, we provide more explicit evidence for their existence by means of *ab initio* simulation of experimental reflectance anisotropy (RA) spectra. Details of the calculation will be given elsewhere [13].

Various experimental RA spectra have been reported in the literature [12,14–16]. In Fig. 4, we reproduce data for MBE-grown and MOCVD-grown samples prepared under very Sb-rich conditions. Clear $c(2 \times 6)$ LEED patterns were observed on the surfaces. Despite some uncertainty in the baseline position, the experimental spectra are very similar, being characterized by a low energy positive peak (identified clearly in the MOCVD-grown sample), a broad negative structure between 1.6 and 3.0 eV, a large peak at 3.7 eV, and a wide trough around the E_2 critical point energy at 4.4 eV. Therefore, the RA spectra should correspond to the same, Sb-rich structural phase.

Our calculated spectra show no agreement for: (i) any stable (4×3) reconstruction, of which we have considered a number of different structures (α, β, γ, $h0$ and staircase variations obtained through shifts of $a/4$ in the alignment of adjacent unit cell rows [17]), or (ii) the $c(4 \times 4)$ reconstruction. The calculated RA spectra of the (4×3) reconstructions show a weak anisotropy at all energies and lack the strong and wide feature present at 3.7 eV. This feature is strongly displaced in energy in the case of the $c(4 \times 4)$ reconstruction. A better agreement with experiment was found for the metallic long-chain $c(2 \times 6)$ structure (dashed line in Fig. 4, top-right panel). The spectrum shows, however, a distinct positive feature between 2.0 and 3.0 eV, in stark contrast with the measured data. Addition of surface Ga antisites (solid lines) causes this positive peak to be systematically *quenched*, while the overall reasonable agreement is maintained. For complete-

ness, we also show RA spectra of the (long-chain) $c(2 \times 10)$ structures, which show similar trends. Hence, we obtain the best overall agreement with the experimental RA data for the surface reconstructions incorporating Ga antisites. A calculation for a different (higher energy) defect configuration yielded a completely negative RA signal in the 1.5–3 eV range [13], demonstrating the sensitivity of RA spectroscopy to the positions of the defects. We note that the defect-stabilized spectra should be further smoothened if a random distribution of defects is considered.

In conclusion, we provide an explanation of why GaSb(001) reconstructions at high Sb coverage feature long chains separated by in-dimers instead of the usual $c(4 \times 4)$ reconstruction formed by almost all other III-V(001) surfaces. Driven by the excess electron surface charge, Ga antisite defects form below the dimer chains that stabilize the long-chain structures and allow the ECR to be fulfilled. This finding suggests ways of engineering the surface reconstruction and therefore the interface structure by means of external probes during growth.

*Corresponding author: conor.hogan@roma2.infn.it
[1] F. Bechstedt, *Principles of Surface Physics* (Springer, Berlin, 2003).
[2] L. J. Whitman *et al.*, Phys. Rev. Lett. **79**, 693 (1997).
[3] U. Resch-Esser *et al.*, Phys. Rev. B **55**, 15401 (1997).
[4] G. E. Franklin *et al.*, Phys. Rev. B **41**, 12619 (1990).
[5] W. Barvosa-Carter *et al.*, Phys. Rev. Lett. **84**, 4649 (2000).
[6] M. T. Sieger *et al.*, Phys. Rev. B **52**, 8256 (1995).
[7] M. C. Righi *et al.*, Phys. Rev. B **71**, 075323 (2005).
[8] O. Romanyuk *et al.*, Phys. Rev. B **79**, 235330 (2009).
[9] Calculations used the PWSCF code [P. Giannozzi *et al.*, J. Phys. Condens. Matter **21**, 395502 (2009)] and a supercell scheme [15 Ry cutoff, (4×6) unit cells with 7-layer-thick slabs (208 atoms), 384 **k**-points in (1×1) Brillouin zone] for all $\times 3$ and $\times 6$ reconstructions. Atoms were relaxed until force components were <2.5 meV/Å.
[10] Guo-Xin Qian *et al.*, Phys. Rev. B **38**, 7649 (1988).
[11] J. Houze *et al.*, Phys. Rev. B **76**, 205303 (2007).
[12] C. Goletti *et al.*, Surf. Sci. **352–354**, 771 (1996). An opposite sign convention was used in this work.
[13] C. Hogan *et al.* (to be published); Denser (∼ 864–1152 **k**-points) meshes and 12-layer slabs (with 152 atoms) were used to compute spectra with the YAMBO code [A. Marini *et al.*, Comput. Phys. Commun. **180**, 1392 (2009)].
[14] K. Möller *et al.*, J. Cryst. Growth **248**, 244 (2003).
[15] Z. Kollonitsch *et al.*, J. Cryst. Growth **261**, 289 (2004).
[16] O. J. Pitts, S. P. Watkins, and C. X. Wang, J. Cryst. Growth **248**, 249 (2003).
[17] O. Romanyuk *et al.*, Phys. Rev. B **77**, 235322 (2008).